World Journal of Advanced Research and Reviews
eISSN: 2581-9615 CODEN (USA): WJARAI
Cross Ref DOI: 10.30574/wjarr
Journal homepage: https://wjarr.com/

(RESEARCH ARTICLE)

Check for updates

Angular Dependence of Magnetosonic and Alfvén Wave Speeds in a Stratified Solar Atmosphere

Chukwudi F. Asara, Chigozie Israel-Cookey, Friday B. Sigalo, Iyeneomie Tamunobereton-ari, Onengiyeofori A. Davies * and Patrick Oki

Department of Physics, Faculty of Science, Rivers State University, Nkpolu-Oroworukwo, Port Harcourt, Rivers State, Nigeria.

World Journal of Advanced Research and Reviews, 2025, 28(02), 832-841

Publication history: Received on 26 September 2025; revised on 03 November 2025; accepted on 06 November 2025

Article DOI: https://doi.org/10.30574/wjarr.2025.28.2.3738

Abstract

This study quantitatively examines the angular dependence of the squared phase speed ratios (v_{ph}^2/v_a^2) for fast and slow magnetosonic waves in a highly gravitationally stratified solar atmosphere. The methodology employed the fundamental MHD governing equations (continuity, momentum, and energy), where the complex, non-linear system was simplified through normalization and subsequent linearization to derive the characteristic dispersion relation, which was then solved numerically using Python. Results for the Fast Magnetosonic Wave (FMSW) show near-unity ratios (≈ 1.0) at parallel propagation in the lower, denser layers (photosphere/chromosphere), but a dramatic, multi-order suppression of the ratio in the upper atmosphere. This suppression is a direct result of the increasing Alfvén speed (v_a) due to decreasing mass density, confirming that FMSW phase speed becomes negligible relative to the background magnetic dynamics in the corona. The most significant finding concerns the Slow Magnetosonic Wave (SMSW), which exhibited large-magnitude negative values for $v_{ph,SMSW}/v_a^2$ across wide oblique angles in the photosphere and chromosphere (e.g., as low as -2060.0 at $\theta = 60°$). The negative v_{ph}^2 confirms that SMSW is predominantly evanescent or strongly damped in the lower atmosphere, suggesting that gravitational stratification effectively prevents this mode from efficiently transporting acoustic energy into the corona. These findings reinforce the crucial role of Alfvén waves as the dominant energy carriers in the upper solar atmosphere and offer new, highly anisotropic diagnostic ratios for solar magneto-seismology, critical for modeling energy flux and improving geomagnetic storm forecasting.

Keywords: Magnetosonic Wave; Alfven Wave; Gravitationally Stratified Solar Atmosphere; Group speed; Numerical Model; Heat transfer

1. Introduction

The outer layers of the Sun, encompassing the chromosphere and corona, represent a plasma environment characterized by extreme thermal and magnetic conditions [1, 2]. Understanding the mechanisms responsible for the immense heating of the solar corona and the acceleration of the solar wind requires a comprehensive theoretical framework, with magneto-hydrodynamic (MHD) waves being a leading candidate for energy transport. MHD wave theory predicts three fundamental modes of propagation in a magnetized plasma: the Alfvén wave and two magneto-acoustic waves, often referred to as fast and slow magnetosonic waves [3, 4]. These modes are instrumental in solar physics, providing diagnostics for plasma conditions through solar magneto-seismology and serving as conduits for mechanical energy from the convective zone into the upper atmosphere.

* Corresponding author: Onengiyeofori A. Davies

A crucial challenge in modeling wave behavior in the Sun is accounting for the inherent non-uniformity of the solar atmosphere [5, 6]. Unlike idealized uniform plasma models, the Sun's atmosphere is fundamentally influenced by gravitational forces, leading to significant density and pressure stratification over small vertical scales [7]. This gravitational stratification profoundly affects the characteristics of wave propagation, including wave speeds, damping, and mode conversion. The relationship between the phase speed (v_{ph}) of the waves, particularly their squared ratio relative to the Alfvén speed (v_a^2), and the angle of propagation (θ) with respect to the background magnetic field is not trivial in such a complex, non-idealized medium [5, 8].

Despite extensive studies into MHD wave characteristics, a rigorous and systematic analysis of the angular dependence of the ratios of squared phase speeds, specifically for the fast and slow magnetosonic modes relative to the Alfvén speed, within a highly gravitationally stratified plasma remains necessary [5, 9]. These ratios act as sensitive indicators of local plasma-β and anisotropic pressures, offering a refined diagnostic tool beyond simple phase speed analysis. The primary objective of the present study is, therefore, to quantitatively examine how the ratio of $v_{\{ph,fast\}}^2$ / v_a^2 and $v_{\{ph,slow\}}^2$ / v_a^2 evolves across the propagation angle in the context of the gravitationally stratified solar atmosphere.

To achieve this goal, we employ the fundamental MHD governing equations, including the equations for mass continuity, momentum, and energy. The complex, non-linear system is simplified through normalization and subsequent linearization, allowing us to derive the characteristic dispersion relation for the waves. This complex algebraic relation is then solved numerically using Python, enabling the systematic calculation of the wave speed ratios for all propagation angles from 0° to 180°.

By mapping the angular dependence of this ratio across a stratified height profile, we aim to provide insight into how wave modes might preferentially propagate or convert in different atmospheric layers, under different magnetic-field inclinations and density gradients. The results have implications for solar wave diagnostics, mode-coupling analyses and potentially for atmospheric heating mechanisms in magnetised plasmas.

2. Material and methods

2.1. Ideal Magnetohydrodynamic (MHD) Equations

Ideal MHD equations describe the motion of a perfectly conducting (ideal) fluid and its interaction with a magnetic field in a uniform atmosphere [10, 11]. They stem from the combination of Maxwell's equations with the equations of gas dynamics. It is assumed that the typical plasma velocities are much less than the speed of light. The MHD equations are the continuity, momentum, energy and diffusion equations as showed in eqns. 1 to 4.

$$\frac{\partial \rho}{\partial t} + \rho \nabla . v = 0 \tag{1}$$

$$\frac{\partial (\rho v)}{\partial t} + \nabla . [(v \rho v - BB)] + \nabla \left[(\gamma - 1) \left(e - \frac{\rho v^2}{2} \right) \right] = \rho g \tag{2}$$

$$\frac{\partial e}{\partial t} + \nabla . (ve - F) + \nabla P = \rho g . v \tag{3}$$

$$\frac{\partial B}{\partial t} + \nabla . (vB - Bv) = 0 \tag{4}$$

The force field is given by;

$$F = BB . v + v(\gamma - 1) \left(e - \frac{\rho v^2}{2} \right) \tag{5}$$

While the pressure field is given by;

$$P = (\gamma - 1) \left(e - \frac{\rho v^2}{2} \right) \tag{6}$$

Where ρ is the mass density, p is the scalar pressure, v is velocity, g is gravity, B is the magnetic field strength, F is the force field, μ_0 is the permeability of free space, e is the energy density and γ is the ratio of specific heats. Owing to this description being of ideal MHD, several terms are absent, such as those encompassing the effects of viscosity, resistivity, hall effects, etc. In any case, these omitted non-ideal terms are considered negligible on the length scales considered within this study.

2.2. Linearized MHD Equations

In order to utilize the MHD equations to study the propagation of magnetosonic or P-waves, we rewrite the system of equations (1) - (4) in terms of an initial time-independent background equilibrium state (p_0, ρ_0, $B_{0,}v_0$**)** and small perturbations (p_1, ρ_1, $B_{1,}v_1$) to that state, such that;.

$$p = p_0 + p_1 \tag{7}$$
$$\rho = \rho_0 + \rho_1 \tag{8}$$
$$B = B_0 + B_1 \tag{9}$$
$$v = v_0 + v_1 \tag{10}$$
$$e = e_0 + e_1 \tag{11}$$

Under static initial conditions; $v_0 = 0$, $\frac{\partial}{\partial t} = 0$, inserting equations 7 – 11 into equations 1 – 4, gives a new set of equations, which are;

$$\frac{\partial \rho_1}{\partial t} + \rho_0 \nabla . v_1 = 0 \tag{12}$$
$$\frac{\partial (\rho_0 v_1)}{\partial t} + \nabla . (2B_0 B_1) + \nabla[(\gamma - 1)\left(e_1 - \frac{\rho_0 {v_1}^2}{2}\right)] = \rho_1 g \tag{13}$$
$$\frac{\partial (e_1)}{\partial t} + \nabla . \left[v_1 e_0 - 2B_0 B_1 v_1 + v_1(\gamma - 1)\left(e_1 - \frac{\rho_0 {v_1}^2}{2}\right)\right] + \nabla(\gamma - 1)\left(e_1 - \frac{\rho_0 {v_1}^2}{2}\right) = \rho_0 g . v_1 \tag{14}$$
$$\frac{\partial B_1}{\partial t} + \nabla . (v_1 B_0 - B_0 v_1) = 0 \tag{15}$$

Assuming wave like solutions of the form $exp\,[i(\boldsymbol{k}\cdot\boldsymbol{r} - \omega t)]$, where $\boldsymbol{k}$ is the wave vector, $\boldsymbol{r}$ contains the spatial coordinates, ω is the angular frequency, and t is time, linearized equations 12 – 15 reduces to ;

$$\omega\rho_1 - \rho_0(k . v_1) = 0 \tag{16}$$
$$\rho_0[i\omega v_1 + (\gamma - 1)(ikv_1)] = \rho_1\left[i(\gamma - 1)k\frac{e_1}{\rho_1} - g\right] \tag{17}$$
$$\begin{aligned} i\omega e_1 + ikv_1 e_1 + ikv_1 e_0 - ik4B_0 B_1 v_1 + (\gamma - 1)\left[2ikv_1 e_1 - i\frac{3}{2}kv_1^2\rho_0 - \frac{1}{2}ikv_1^3\rho_1\right] \\ + (\gamma - 1)\left[ike_1 - ik\rho_0 v_1 - ik\frac{1}{2}v_1^2\rho_1\right] = \rho_0 g . v_1 \end{aligned} \tag{18}$$
$$-iwB_1 = B_0 ikv_1 - B_0 ikv_1 \tag{19}$$

Under the assumption that $\omega \neq 0$, equations (2.16) - (2.19) yield the solutions,

$$\rho_1 = \rho_0\frac{k . v_1}{\omega} \tag{20}$$
$$\frac{\rho_0}{\rho_1} = \frac{\left[i(\gamma - 1)k\frac{e_1}{\rho_1} - g\right]}{[i\omega v_1 + (\gamma - 1)(ikv_1)]} \tag{21}$$
$$\begin{aligned} \rho_0\left[i\frac{3}{2}kv_1^2 + ikv_1\right] = ik4B_0 B_1 v_1 - \frac{(i\omega e_1 + ikv_1 e_1 + ikv_1 e_0)}{(\gamma - 1)} - \left[\frac{1}{2}ikv_1^3\rho_1 + ik\frac{1}{2}v_1^2\rho_1\right] + \\ [2ikv_1 e_1 + ike_1] - \frac{g . v_1}{(\gamma - 1)} \end{aligned} \tag{22}$$
$$-iwB_1 = 0 \tag{23}$$

According to Goedbloed and Poedts [12], in the case of a non-zero magnetic field and without loss of generality, the equilibrium magnetic field B_0 can be directed along the z-axis with the wave vector $\boldsymbol{k}$ lying in the x – z plane. Representing the linearized equation in matrix form, we have;

$$\begin{bmatrix} \omega^2 - k^2{v_a}^2 - k^2{v_s}^2 sin^2\theta & 0 & -k^2{v_s}^2\sin\theta\cos\theta \\ 0 & \omega^2 - k^2{v_a}^2 cos^2\theta & 0 \\ -k^2{v_s}^2\sin\theta\cos\theta & 0 & \omega^2 - k^2{v_s}^2 cos^2\theta \end{bmatrix}\begin{bmatrix} v_x \\ v_y \\ v_z \end{bmatrix} = 0 \tag{24}$$

Here, the subscripts for the perturbation velocity have been dropped and replaced with their respective cartesian coordinates, θ is defined as the angle between B_0 and k, $k = |k|$. The Alfvén speed and sound speed can thus be expressed as;

$$v_a = \sqrt{\frac{B_0^2}{\mu_0 \rho_0}} \tag{25}$$

$$v_s = \sqrt{\frac{\gamma p_0}{\rho_0}} \tag{26}$$

Solutions to equation (24) exist only when the determinant of the left-hand square matrix is zero, which in turn provides the dispersion relation.

$$(\omega^2 - k^2 {v_a}^2 cos^2\theta)[\omega^4 - \omega^2 k^2({v_a}^2 + {v_s}^2) + k^4 {v_a}^2 {v_s}^2 cos^2\theta] = 0 \tag{27}$$

There are three independent real roots of the above dispersion relation, which correspond to the three different types of waves that can propagate through an MHD medium.

The first of these roots describes the shear Alfvén wave and is expressed as;

$$\omega = k v_a \cos\theta \tag{28}$$

This wave involves plasma motion strictly perpendicular to the magnetic field, a fact which can be seen through equations (20) and (21), which reveal zero perturbation to the density or pressure. The remaining two roots of the dispersion relation are gotten by solving quadratically the bi-quadratic equation using the formula,

$$[\omega^4 - \omega^2 k^2({v_a}^2 + {v_s}^2) + k^4 {v_a}^2 {v_s}^2 cos^2\theta] = 0 \tag{29}$$

$$\omega^2 = P \tag{30}$$

$$C_{ms} = \pm\sqrt{(v_a^2 + v_s^2)} \tag{31}$$

Where C_{ms} is the magnetosonic speed. Inserting equations (30) and (31) into equation (29), we have

$$[(\omega^2)^2 - \omega^2 k^2 C_{ms}^2 + k^4 {v_a}^2 {v_s}^2 cos^2\theta] = 0 \tag{32}$$

$$[(P)^2 - P k^2 C_{ms}^2 + k^4 {v_a}^2 {v_s}^2 cos^2\theta] = 0 \tag{33}$$

Recall that a quadratic equation is generally defined as $aP^2 + bP + c = 0$. From equation (33), $a = 1$, $b = -k^2 C_{ms}^2$ and $c = k^4 {v_a}^2 {v_s}^2 cos^2\theta$. According to the almighty formular,

$$P = \frac{2c}{-b \pm \sqrt{b^2 + 4ac}} \tag{34}$$

Inserting equation (30) and values of a, b and c into equation (34),

$$\omega^2 = \frac{2k^4 {v_a}^2 {v_s}^2 cos^2\theta}{k^2 C_{ms}^2 + \sqrt{k^4 (C_{ms}^2)^2 + 4k^4 {v_a}^2 {v_s}^2 (1 - sin^2\theta)}} \tag{35}$$

From equation (35), we obtain two dispersion relations which are,

$$\omega^2 = \frac{2k^4 {v_a}^2 {v_s}^2 cos^2\theta}{k^2 C_{ms}^2 + \sqrt{k^4 (C_{ms}^2)^2 + 4k^4 {v_a}^2 {v_s}^2 (1 - sin^2\theta)}} \tag{36}$$

$$\frac{\omega^2}{k^2} = \frac{2{v_a}^2 {v_s}^2 (1 - sin^2\theta)}{C_{ms}^2 \pm \sqrt{(C_{ms}^2)^2 + 4{v_a}^2 {v_s}^2 (1 - sin^2\theta)}} \tag{37}$$

$$v_{ph}^2 = \frac{2{v_a}^2 {v_s}^2 (1 - sin^2\theta)}{C_{ms}^2 \pm \sqrt{(C_{ms}^2)^2 + 4{v_a}^2 {v_s}^2 (1 - sin^2\theta)}} \tag{38}$$

$$v_{Ph,FMSW}^2 = \frac{2{v_a}^2 {v_s}^2 (1 - sin^2\theta)}{C_{ms}^2 + \sqrt{(C_{ms}^2)^2 + 4{v_a}^2 {v_s}^2 (1 - sin^2\theta)}} \tag{39}$$

$$v_{ph,SMSW}^2 = \frac{2{v_a}^2 {v_s}^2 (1 - sin^2\theta)}{C_{ms}^2 - \sqrt{(C_{ms}^2)^2 + 4{v_a}^2 {v_s}^2 (1 - sin^2\theta)}} \tag{40}$$

Where v_{Ph} is the phase speed, C_{ms} is the magnetosonic speed, v_a is the Alfven speed, v_s is the sound speed, fast magnetosonic wave (FMSW) and slow magnetosonic wave (SMSW). Here, the fast and slow magnetosonic wave mode corresponds to the positive and negative solutions, respectively, of equation (38). These waves have non-zero perturbations to the density and pressure and involve plasma motion both perpendicular and parallel to the magnetic field.

2.3. Astrophysical Constants

Certain astrophysical constants were required to estimate v_a and v_s. These constants are shown in table 1 below.

Table 1 Selected Astrophysical Constants for Solar Atmosphere [13]

Solar Atmosphere	Stratified /Layers	Magnetic Field (B_0)(G)	Mass Density (ρ_0)(Kgm^{-3})
Photosphere	Lower	500 - 2000	1.65×10^{-6}
	Mid		1.4×10^{-8}
	Upper		5.5×10^{-6}
Chromosphere	Lower	1 - 500	3.75×10^{-10}
	Mid		2.25×10^{-11}
	Upper		7.5×10^{-12}
Corona	Lower	0.1 - 10	3.0×10^{-13}
	Mid		1.25×10^{-13}
	Upper		3.0×10^{-15}

3. Results

The evaluated ratios of the square of phase speed of the fast and slow magnetosonic waves to Alfven speed with the propagation angle in a highly gravitationally stratified solar atmosphere are presented in tables (2) to (4), while a curve of the ratio of phase speed of fast and slow magnetosonic waves against angle of propagation is presented in fures (1) to (3):

Table 2 Estimated Ratio of the Square of Phase Speed of the Fast and Slow Magnetosonic Waves to Alfven Speed with the Propagation Angle in a Highly Gravitationally Stratified Solar Photosphere

Propagation Angle	Lower Photosphere		Mid Photosphere		Upper Photosphere	
	$\left(\frac{v_{ph,FMSW}}{v_a}\right)^2$	$\left(\frac{v_{ph,SMSW}}{v_a}\right)^2$	$\left(\frac{v_{ph,FMSW}}{v_a}\right)^2$	$\left(\frac{v_{ph,SMSW}}{v_a}\right)^2$	$\left(\frac{v_{ph,FMSW}}{v_a}\right)^2$	$\left(\frac{v_{ph,SMSW}}{v_a}\right)^2$
0	0.999	−0.205	0.431	−2.47	0.372	−2.17
45	0.707	−2050.0	0.234	−2.28	0.202	−1.99
60	0.250	−2060.0	0.123	−2.52	0.106	−0.98
135	0.707	−2050.0	0.234	−2.28	0.202	−1.99
180	0.999	−0.205	0.431	−2.47	0.372	−2.17

Table 3 Estimated Ratio of the Square of Phase Speed of the Fast and Slow Magnetosonic Waves to Alfven Speed with the Propagation Angle in a Highly Gravitationally Stratified Solar Chromosphere

Propagation Angle	Lower Chromosphere		Mid Chromosphere		Upper Chromosphere	
	$\left(\frac{v_{ph,FMSW}}{v_a}\right)^2$	$\left(\frac{v_{ph,SMSW}}{v_a}\right)^2$	$\left(\frac{v_{ph,FMSW}}{v_a}\right)^2$	$\left(\frac{v_{ph,SMSW}}{v_a}\right)^2$	$\left(\frac{v_{ph,FMSW}}{v_a}\right)^2$	$\left(\frac{v_{ph,SMSW}}{v_a}\right)^2$
0	0.992	−667.0	0.983	−149.0	3.02×10^{-7}	−0.972
45	0.497	−666.0	0.493	−297.0	1.51×10^{-7}	−0.971
60	0.248	−666.0	0.247	−134.0	75.0×10^{-7}	−0.974
135	0.497	−666.0	0.493	−297.0	1.51×10^{-7}	−0.971
180	0.992	−667.0	0.983	−149.0	3.02×10^{-7}	−0.972

Table 4 Estimated Ratio of the Square of Phase Speed of the Fast and Slow Magnetosonic Waves to Alfven Speed with the Propagation Angle in a Highly Gravitationally Stratified Solar Corona

Propagation Angle	Lower Corona		Mid Corona		Upper Corona	
	$\left(\frac{v_{ph,FMSW}}{v_a}\right)^2$	$\left(\frac{v_{ph,SMSW}}{v_a}\right)^2$	$\left(\frac{v_{ph,FMSW}}{v_a}\right)^2$	$\left(\frac{v_{ph,SMSW}}{v_a}\right)^2$	$\left(\frac{v_{ph,FMSW}}{v_a}\right)^2$	$\left(\frac{v_{ph,SMSW}}{v_a}\right)^2$
0	0.00466	−1.02	0.00289	−1.01	0.00260	−0.010
45	0.00233	−1.01	0.00145	−1.00	0.00130	−1.003
60	0.11700	−1.04	0.00073	−1.00	0.00065	−1.010
135	0.00233	−1.01	0.00145	−1.01	0.00130	−1.003
180	0.00466	−1.02	0.00289	−1.01	0.00260	−1.005

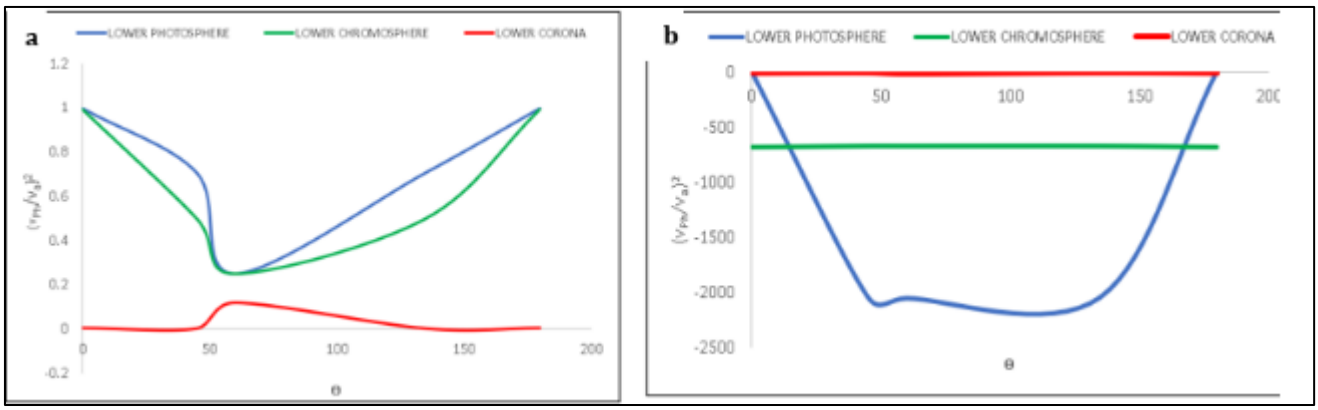

Figure 1 A curve of the ratio of the square of phase speed of (a) fast magnetosonic wave to Alfven wave speed against angle of propagation in lower solar atmosphere (b) slow magnetosonic wave to Alfven wave speed against angle of propagation in lower solar atmosphere

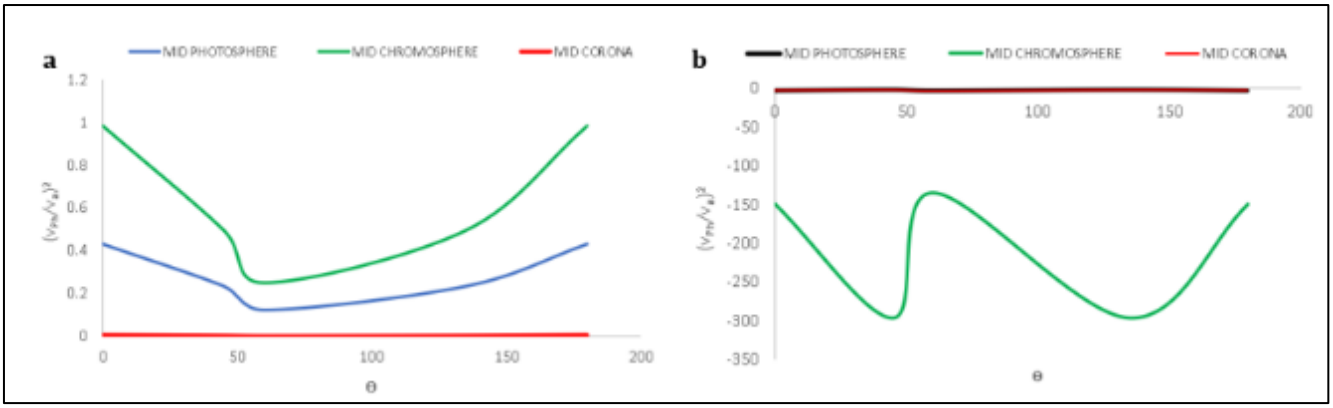

Figure 2 A curve of the ratio of the square of phase speed of (a) fast magnetosonic wave to Alfven wave speed against angle of propagation in mid solar atmosphere (b) slow magnetosonic wave to Alfven wave speed against angle of propagation in mid solar atmosphere

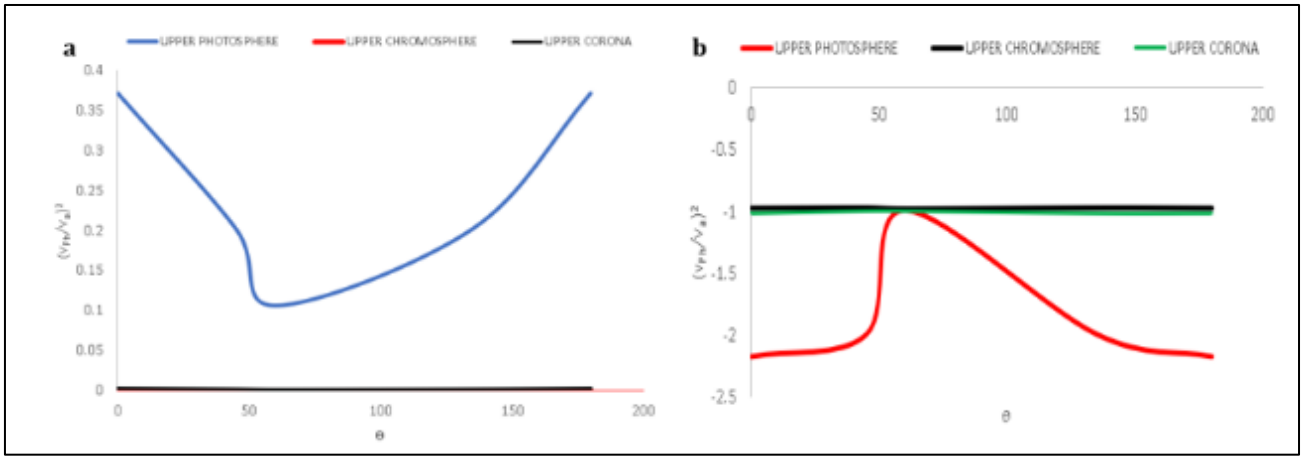

Figure 3 A curve of the ratio of the square of phase speed of (a) fast magnetosonic wave to Alfven wave speed against angle of propagation in upper solar atmosphere (b) slow magnetosonic wave to Alfven wave speed against angle of propagation in upper solar atmosphere

4. Discussion

The results presented in the preceding tables provide a detailed quantitative characterization of the angular dependence of wave speed ratios (v_{ph}^2/v_a^2) for fast magnetosonic waves (FMSW) and slow magnetosonic waves (SMSW) across various regions of the gravitationally stratified solar atmosphere, from the photosphere to the corona. These findings illuminate the profound influence of density and temperature gradients on energy propagation and mode characteristics. Analysis of the FMSW ratio, $V_{ph,\mathrm{FMSW}}^2/v_a^2$, consistently demonstrates a maximal value at $\theta = 0°$ and $180°$ (parallel propagation) across all atmospheric layers. According to Nakariakov and Verwichte [14], this behavior is characteristic of the fast mode, where phase speed is highest when propagating along the magnetic field lines. In the lower atmosphere, specifically the lower photosphere, lower chromosphere, and mid chromosphere, the ratio approaches unity (e.g., 0.999, 0.992, and 0.983 at parallel propagation). This proximity to 1.0 suggests that in these denser, cooler regions, the thermal speed (C_{ms}) is relatively low compared to the Alfvén speed, causing the FMSW to predominantly behave like a non-compressive Alfvén wave when traveling parallel to the field [14, 15]. As the propagation angle increases to $\theta = 45°$, the FMSW ratio drops significantly, exhibiting the characteristic $cos^2\theta$ dependency expected from standard MHD theory for the fast mode.

However, a striking transition occurs upon moving to the upper chromosphere and corona. Here, the FMSW ratios are orders of magnitude smaller (e.g., maximum of 3.02×10^{-7} in the upper chromosphere, and 0.00466 in the lower corona). This dramatic reduction is the direct consequence of the sharp drop in mass density and the subsequent increase in the Alfvén speed (v_a), which is inversely proportional to the square root of density. Because the phase speed v_{ph} is constrained by the local background conditions, the massive relative increase in v_a due to stratification causes

the ratio $v_{ph,\mathrm{FMSW}}^2 / v_a^2$ to plummet. This indicates that while the FMSW exists in the upper atmosphere, its phase speed becomes less influential relative to the background Alfvén speed in the highly tenuous, magnetically dominated upper layers [16, 17].

The most notable and theoretically significant finding is the highly unusual, large-magnitude negative values obtained for the SMSW ratio, $v_{ph,\mathrm{SMSW}}^2/v_a^2$, particularly in the denser layers of the photosphere and chromosphere. A negative value for the squared phase speed indicates that the corresponding wave mode is evanescent or non-propagating in the direction examined, meaning the energy associated with the SMSW is not transferred via standard propagating oscillations but is instead exponentially damped or trapped [14, 18]. The extremely large negative magnitudes (e.g., -2060.0 at $\theta = 60°$ in the lower photosphere) highlight a highly constrained or resonant regime. This prevalence of large negative values in the lower atmosphere suggests that the combined effects of strong gravitational stratification and the large pressure gradients overwhelm the magnetic restoring force for the slow mode in certain directions, according to Yu *et. al.* [19]. Specifically, the sharp, angle-dependent spike to -2060.0 at $\theta = 60°$ in the lower photosphere suggests that waves entering the solar atmosphere obliquely are immediately damped or reflect strongly due to the stiffening effect of the density gradient. The large negative values persist up through the mid chromosphere (e.g., -297.0 at $45° / 135°$), confirming that the SMSW is predominantly non-propagating in these gravitationally stressed regions for a significant range of angles. In contrast to the complex behavior below, the SMSW ratio in the corona stabilizes around a much smaller magnitude, near -1.0 (e.g., -1.01 to -1.02). While still indicating an evanescent wave, the magnitude is now far smaller and more predictable, suggesting that in the high-Alfvén speed, low-β coronal plasma, the wave is damped more uniformly, unlike the complex trapping/damping seen in the lower atmosphere [20, 21].

The highly anisotropic nature of both FMSW and SMSW demonstrated by this angular analysis has critical implications for coronal heating and solar wind acceleration: the significant damping and evanescent behavior of the SMSW in the chromosphere suggests this mode is unlikely to be an efficient large-scale transporter of acoustic energy to power the solar corona, meaning its energy is likely dissipated rapidly (mode-converted to heat) within the transition region [22, 23]. Conversely, the extreme values of v_a implied by the very low $v_{ph,\mathrm{FMSW}}^2/v_a^2$ ratios in the corona strongly support the hypothesis that Alfvén waves are the dominant and most efficient movers of energy in the upper solar atmosphere [24, 25]. Their incompressible nature and lack of dependence on sound speed make them robust against gravitational stratification, supporting the long-standing recommendation that their large group speed is crucial for optimizing energy transfer from the stellar interior into the corona, thereby driving the stellar wind. Furthermore, the highly angle-dependent and distinct values of $v_{ph,\mathrm{FMSW}}^2/v_a^2$ and $v_{ph,\mathrm{SMSW}}^2/v_a^2$ across the different atmospheric layers provide a potential new diagnostic tool for solar magneto-seismology, allowing for a correlation between precise wave measurements at the photosphere and the specific phase speed ratios derived here. This correlation could lead to more accurate modeling of energy flux emergence, which ultimately impacts the intensity and characteristics of interplanetary disturbances relevant to space weather and geomagnetic storm forecasting.

5. Conclusion

This study successfully quantified the angular dependence of the squared phase speed ratios for fast and slow magnetosonic waves (v_{ph}^2/v_a^2) across the highly gravitationally stratified solar atmosphere, from the photosphere to the corona. Using the fundamental MHD equations for mass continuity, momentum, and energy, we developed a theoretical model in which the complex, non-linear system was simplified through normalization and linearization to obtain the characteristic dispersion relation. The results provide critical insight into how density and pressure gradients fundamentally alter the classical behavior of these plasma wave modes, offering refined diagnostics for solar energy transport mechanisms. Numerical analysis of this relation across photospheric, chromospheric, and coronal layers revealed several key results:

- The fast magnetosonic to Alfvén speed ratio is largest for propagation parallel to the magnetic field and decreases markedly at oblique angles, showing that angular dependence strongly governs wave-mode interactions.
- The slow magnetosonic wave ratio varies irregularly with angle and height, indicating increased sensitivity to local plasma β and density gradients.
- Gravitational stratification enhances Alfvénic dominance in the upper atmosphere, as the Alfvén speed rises rapidly with decreasing density, while sound speed remains comparatively low.
- The observed angular trends imply that wave coupling and energy redistribution are most efficient at intermediate propagation angles, supporting theories that link Alfvénic perturbations to coronal heating and solar wind acceleration.

Overall, the analysis demonstrates that the combined effects of propagation angle and gravitational stratification are key to understanding MHD wave behavior in the solar atmosphere. Future work should extend this approach to include dissipative effects, nonlinear coupling, and magnetic field divergence to better quantify energy transport from the photosphere to the corona.

Compliance with ethical standards

Acknowledgements

The authors gratefully acknowledge the support of the Authorities of Rivers State University, Port Harcourt, Rivers State, Nigeria.

Disclosure of conflict of interest

All authors declare that there are no conflicts of interest regarding this paper publication.

References

[1] De Moortel, I. and P. Browning, *Recent advances in coronal heating.* Philosophical Transactions of the Royal Society A: Mathematical, Physical Engineering Sciences, 2015. 373(2042): p. 20140269.

[2] Alissandrakis, C.E. and D.E. Gary, *Radio measurements of the magnetic field in the solar chromosphere and the corona.* Frontiers in Astronomy and Space Sciences, 2021. 7: p. 591075.

[3] Zhao, S., C. Xiao, X. Wang, Z. Pu, M. Shi, and T. Liu, *Observation of a large-amplitude slow magnetosonic wave in the magnetosheath.* Journal of Geophysical Research: Space Physics, 2019. 124(12): p. 10200-10208.

[4] Zhao, L., X. Zhu, A. Silwal, G.P. Zank, and A. Pitňa, *Theory and observations of the interaction between magnetohydrodynamic waves and shocks.* Proceedings of the National Academy of Sciences, 2025. 122(20): p. e2425668122.

[5] Goossens, M.L., I. Arregui, and T. Van Doorsselaere, *Mixed properties of MHD waves in non-uniform plasmas.* Frontiers in Astronomy and Space Sciences, 2019. 6: p. 20.

[6] Erdélyi, R. and N.K. Zsámberger, *Magnetohydrodynamic waves in asymmetric waveguides and their applications in solar physics—a review.* Symmetry, 2024. 16(9).

[7] Alissandrakis, C.E., *Structure of the solar atmosphere: a radio perspective.* Frontiers in Astronomy and Space Sciences, 2020. 7: p. 574460.

[8] Erdélyi, R., K. Al-Ghafri, and R. Morton, *Damping of longitudinal magneto–acoustic oscillations in slowly varying coronal plasma.* Solar Physics, 2011. 272(1): p. 73.

[9] Nakariakov, V.M., S. Zhong, D.Y. Kolotkov, R.L. Meadowcroft, Y. Zhong, and D. Yuan, *Diagnostics of the solar coronal plasmas by magnetohydrodynamic waves: magnetohydrodynamic seismology.* Reviews of Modern Plasma Physics, 2024. 8(1): p. 19.

[10] Cally, P.S. and T.J. Bogdan, *MHD waves in homogeneous and continuously stratified atmospheres*, in *Magnetohydrodynamic Processes in Solar Plasmas*. 2024, Elsevier. p. 99-153.

[11] Palenzuela, C., L. Lehner, O. Reula, and L. Rezzolla, *Beyond ideal MHD: towards a more realistic modelling of relativistic astrophysical plasmas.* Monthly Notices of the Royal Astronomical Society and Astronomical Society, 2009. 394(4): p. 1727-1740.

[12] Goedbloed, J.H. and S. Poedts, *Principles of magnetohydrodynamics: with applications to laboratory and astrophysical plasmas*. 2004: Cambridge university press.

[13] Aschwanden, M., *Physics of the Solar Corona—An Introduction*. 2004, Praxis Publishing Ltd. and Springer: Chichester United Kingdom.

[14] Nakariakov, V.M. and E. Verwichte, *Coronal waves and oscillations.* Living Reviews in Solar Physics, 2005. 2(1): p. 3.

[15] Roberts, B., *MHD waves in the solar atmosphere*. 2019: Cambridge University Press.

[16] Nakariakov, V. and B. Roberts, *Magnetosonic waves in structured atmospheres with steady flows: I. Magnetic slabs.* Solar Physics, 1995. 159(2): p. 213-228.

[17] Wright, A. and T. Elsden, *Resonant fast-Alfvén wave coupling in a 3D coronal arcade.* Physics, 2023. 5(1): p. 310-321.

[18] Goossens, M., J. Terradas, J. Andries, I. Arregui, and J.L. Ballester, *On the nature of kink MHD waves in magnetic flux tubes.* Astronomy & Astrophysics, 2009. 503(1): p. 213-223.

[19] Yu, D., T. Van Doorsselaere, and M. Goossens, *Resonant absorption of the slow sausage wave in the slow continuum.* Astronomy & Astrophysics, 2017. 602: p. A108.

[20] Nakariakov, V., S. Anfinogentov, P. Antolin, R. Jain, D. Kolotkov, E. Kupriyanova, D. Li, N. Magyar, G. Nisticò, and D. Pascoe, *Kink oscillations of coronal loops.* Space Science Reviews, 2021. 217(6): p. 73.

[21] Ruderman, M. and B. Roberts, *The damping of coronal loop oscillations.* The Astrophysical Journal, 2002. 577(1): p. 475.

[22] Cally, P.S., *Alfvén reflection and reverberation in the solar atmosphere.* Solar Physics, 2012. 280(1): p. 33-50.

[23] Erdélyi, R., C. Malins, G. Tóth, and B. De Pontieu, *Leakage of photospheric acoustic waves into non-magnetic solar atmosphere.* Astronomy & Astrophysics, 2007. 467(3): p. 1299-1311.

[24] Tomczyk, S., S. McIntosh, S. Keil, P. Judge, T. Schad, D. Seeley, and J. Edmondson, *Alfvén waves in the solar corona.* Science, 2007. 317(5842): p. 1192-1196.

[25] McIntosh, S.W., B. De Pontieu, M. Carlsson, V. Hansteen, P. Boerner, and M. Goossens, Alfvénic waves with sufficient energy to power the quiet solar corona and fast solar wind. Nature, 2011. 475(7357): p. 477-480.